Brain Struct Funct (2017) 222:71–81
DOI 10.1007/s00429-016-1201-5

ORIGINAL ARTICLE

Anatomic characterization of prelemniscal radiations by probabilistic tractography: implications in Parkinson's disease

María Guadalupe García-Gomar[1] · Julian Soto-Abraham[2] · Francisco Velasco-Campos[2] · Luis Concha[1]

Received: 2 July 2015 / Accepted: 9 February 2016 / Published online: 22 February 2016

Abstract To characterize the anatomical connectivity of the prelemniscal radiations (Raprl), a white matter region within the posterior subthalamic area (PSA) that is an effective neurosurgical target for treating motor symptoms of Parkinson's disease (PD). Diffusion-weighted images were acquired from twelve healthy subjects using a 3T scanner. Constrained spherical deconvolution, a method that allows the distinction of crossing fibers within a voxel, was used to compute track-density images with sufficient resolution to accurately delineate distinct PSA regions and probabilistic tractography of Raprl in both hemispheres. Raprl connectivity was reproducible across all subjects and showed fibers traversing through this region towards primary and supplementary motor cortices, the orbitofrontal cortex, ventrolateral thalamus, and the globus pallidus, cerebellum and dorsal brainstem. All brain regions reached by Raprl fibers are part of motor circuits involved in the pathophysiology of PD; while these fiber systems converge at the level of the PSA, they can be spatially segregated. Fibers of distinct and specific motor control networks are identified within Raprl. The description of this anatomical crossroad suggests that, in the future, tractography could allow deep brain stimulation or lesional therapies in white matter targets according to individual patient's symptoms.

Keywords Parkinson's disease · Prelemnsical radiations · Constrained spherical deconvolution · Track-density images · Probabilistic tractography

Introduction

PD is a progressive neurodegenerative disease characterized by motor and non-motor symptoms. When tremor, rigidity and bradykinesia (the cardinal motor symptoms of the disease) become incapacitating and cannot be controlled by medication, surgical alternatives are required.

In 1962 Spiegel and Wycis proposed to treat PD symptoms by lesioning the H2 Forel's Field to interrupt pallidal and cerebellar fibers to the thalamus (Spiegel et al. 1962). Andy et al. reported in 1963 that subthalamic lesions at the side of the red nucleus (perirubral fibers) controlled rest and intention tremor (Andy et al. 1963). In 1965 Mundinger noted that small lesions below ventrolateral thalamus (VL) thalamic nucleus produced long lasting and better control of tremor and rigidity than large lesions in the thalamic and pallidal targets (Mundinger 1965). The posterior subthalamic area (PSA) was proposed in 1969 as the optimum target for tremor, because the simple introduction of an electrode in this area could stop contralateral tremor (Bertrand et al. 1969). Later, the anatomical substrate where this effect is induced was defined as the prelemniscal radiations (Raprl), an area of fibers located anterior to the medial lemniscus, lateral to the red nucleus (Ru), posterior and medial to the internal

F. Velasco-Campos and L. Concha have contributed equally to this work.

Electronic supplementary material The online version of this article (doi:10.1007/s00429-016-1201-5) contains supplementary material, which is available to authorized users.

✉ Luis Concha
lconcha@unam.mx

[1] Instituto de Neurobiología, Universidad Nacional Autónoma de México, Querétaro, México

[2] Unit for Stereotactic and Functional Neurosurgery and Radiosurgery, Mexico General Hospital, Mexico City, Mexico

border of the subthalamic nucleus (STN) and medial to the caudal zona incerta (Zic) in the anatomic atlas of Schaltenbrand and Wahren (Velasco and Velasco 1979; Velasco et al. 1972). Intra-operative electrophysiological recordings show that Raprl is composed of white matter (Jiménez et al. 2000). Deep brain stimulation (DBS) of Raprl was initially used to treat tremor and rigidity in PD cases with predominant acral symptoms (Kitagawa et al. 2005; Murata et al. 2003; Velasco et al. 2001). A few years later, patients with severe bradykinesia and postural disturbances were unsuccessfully treated with bilateral Raprl-DBS (Carrillo-Ruiz et al. 2008) which showed that Raprl-DBS can only ameliorate the symptomatic triad of the disease. Previous efforts to elucidate the optimum location for PSA-DBS for treating tremor of diverse etiology showed that the largest therapeutic effects are seen with the stimulation at the interface between STN, Zic and Raprl (Velasco et al. 1972; Velasco and Velasco 1979; Blomstedt et al. 2009; Blomstedt et al. 2011; Hamel et al. 2007; Herzog et al. 2007; Kitagawa et al. 2005; Murata et al. 2003; Plaha et al. 2004; Sandvik et al. 2012; Volkmann 2004).[1]

The STN has been extensively utilized as a target for DBS to treat PD (Voges et al. 2002; Hamel et al. 2003; Herzog et al. 2004; Wichmann and Delong 2011), and for this reason its anatomy, connectivity, stereotactic localization and electrophysiology have been thoroughly studied. On the other hand, despite the proven efficacy of Raprl-DBS, this white matter crossroad remains understudied. The purpose of this report is to describe different fiber populations that compose the Raprl in humans using high angular resolution, diffusion-weighted MRI (DWI) and probabilistic tractography.

Materials and methods

Participants

We studied twelve right-handed subjects (7 females), with ages between 42 and 60 (50 ± 5.7) years, without clinical or MRI evidence of neurological disorders and without family history of PD or psychiatric disorders. Participants were evaluated with the Edinburgh Handedness Inventory (Oldfield 1971) and the Symptom Check List-90 (SCL-90) (Derogatis et al. 1976). The Institutional Review Board of the Institute of Neurobiology approved the protocol, and written informed consent was obtained from all participants in accordance with the Declaration of Helsinki.

[1] Care must be taken when studying the available literature, as there are historical discrepancies between studies on the nomenclature of DBS and lesions of the subthalamic and posterior subthalamic areas, and on occasions there is insufficient data to prove that DBS is targeting either region exclusively.

MRI data acquisition

Images were obtained with a 3T Philips Achieva TX MRI scanner (Philips Medical Systems, Best, the Netherlands) located at the Institute of Neurobiology in Queretaro, Mexico. All images were acquired with a 32-channel head coil. High resolution T1-weighted images were acquired using a 3D fast gradient echo sequence with a spatial resolution of $1 \times 1 \times 1$ mm^3 with TR/TE = 8.05/3.68 ms; T2FLAIR images were acquired on the sagittal plane using a 3D turbo-spin echo sequence with in-plane resolution of 1×1 mm^3, 1.12 mm slice thickness and 0.56 mm inter-slice gap with TR/TI/TE = 4800/1650/279 ms.

High angular resolution DWI were acquired with a resolution of $2 \times 2 \times 2$ mm^3, with 65 contiguous slices that provided full brain coverage, and 120 unique diffusion-gradient directions ($b = 2000$ s/mm^2) that were uniformly distributed in space, along with four non-DWI ($b = 0$ s/mm^2). Scan time was around 50 min per subject.

Preprocessing

DWI were processed for eddy-current distortions by registering each volume to the first non-DWI via a linear transformation with 12 degrees of freedom using *fsl* tools (v.4.1.9, FMRIB software library). The diffusion gradient vectors were rotated accordingly (Leemans and Jones 2009).

Fiber-tracking

We used the MRtrix software package (version 0.2.12, Brain Research Institute, Melbourne, Australia, http://www.brain.org.au/software/) to model multiple fiber populations within a voxel by constrained spherical deconvolution (CSD) (Tournier et al. 2007). Fiber orientation distributions (FOD) in each voxel were estimated with a harmonic order of 12 (Tournier et al. 2007, 2008, 2012). Fiber-tracking was based on the probabilistic streamlines method (Behrens et al. 2003) and was performed using the following parameters: 0.2 mm step-size, maximum angle between steps = 12°, minimum radius of curvature = 1 mm.

Track-density images (TDI)

Probabilistic tractography for generating TDI maps was performed in the whole brain. A total of one million tracks were generated throughout the white matter, from which we computed track visitation counts with a spatial resolution of $0.2 \times 0.2 \times 0.2$ mm^3, also known as super-resolution imaging or TDI (Calamante et al. 2010). This method exploits the redundant information obtained by

tractography results and allows the generation of maps with higher spatial resolution than the acquired data.

Image fusion and reorientation

T1 and T2FLAIR volumes were co-registered to the subject's non-DWI ($b = 0$ s/mm^2) by a non-linear deformation using the Advanced Normalization Tools (ANTS, http://www.picsl.upenn.edu/ANTS/). Finally, all images were reoriented to the AC-PC line using a rigid-body transformation in order to match the orientation of the Schaltenbrand and Wahren atlas.

Image segmentation

The STN exhibits large anatomical variability and age-related changes (den Dunnen and Staal 2005; Forstmann et al. 2012; Keuken et al. 2013; Kitajima et al. 2008; Massey et al. 2012). Thus, delimitation of the STN and its anatomic relationships with nearby structures cannot be reliably performed in an automated fashion. In this work manual segmentation of the STN, Ru, zona incerta (Zi) and Raprl was performed jointly by two examiners (MGGG and FVC) based on the co-registered TDI and T2FLAIR volumes aided by the Schaltenbrand-Wahren atlas (Schaltenbrand and Wahren 1977). Segmentations were corroborated in axial, coronal and sagittal brain views (Fig. 1). In T2FLAIR the STN was visualized as a small, almond-shaped hypo-intensity lateral to the anterior edge of the Ru, while in TDI it appears as a black region. Ru, in the midbrain tegmentum, is round and is located lateral to the third ventricle. In each hemisphere Zi and Raprl are located between the STN and Ru, and the posterior arm of the internal capsule and the medial lemniscus are their postero-lateral limits, with Forel's fields being their medial-anterior boundary. Given that the limit between Raprl and Zi is unclear especially in its caudal part (Kerl et al. 2012, 2013) and that boundaries between these structures could not be clearly visualized, their limits were based on the Schaltenbrand-Wahren atlas.

Probabilistic tractography

Probabilistic diffusion tractography was performed in subject-specific space, seeding 50,000 streamlines within Raprl per hemisphere to generate a connectivity probability distribution into every voxel in the brain. For a careful and accurate dissection of the resulting connectivity, target structures were identified by means of an automated anatomical labeling atlas (Desikan-Killiany Atlas), as implemented by *freesurfer* (v.5.3, http://surfer.nmr.mgh.harvard.edu). To simplify further analyses, we grouped cortical target regions of interest into greater anatomical areas (subsequently called target ROIs): (a) Orbitofrontal cortex (OFC), including lateral and medial orbitofrontal cortex; (b) Prefrontal cortex (PFC), which comprises the frontal pole, pars orbitalis, pars triangularis and rostral middle frontal gyrus; (c) Supplementary motor area (SMA), corresponding to the superior interhemispheric frontal gyrus; (d) Primary motor cortex (PMC) matching the precentral gyrus (Supplementary Figure 1). Cerebellum was divided into hemispheres, and each one was manually segmented into deep gray nuclei and cerebellar cortex.

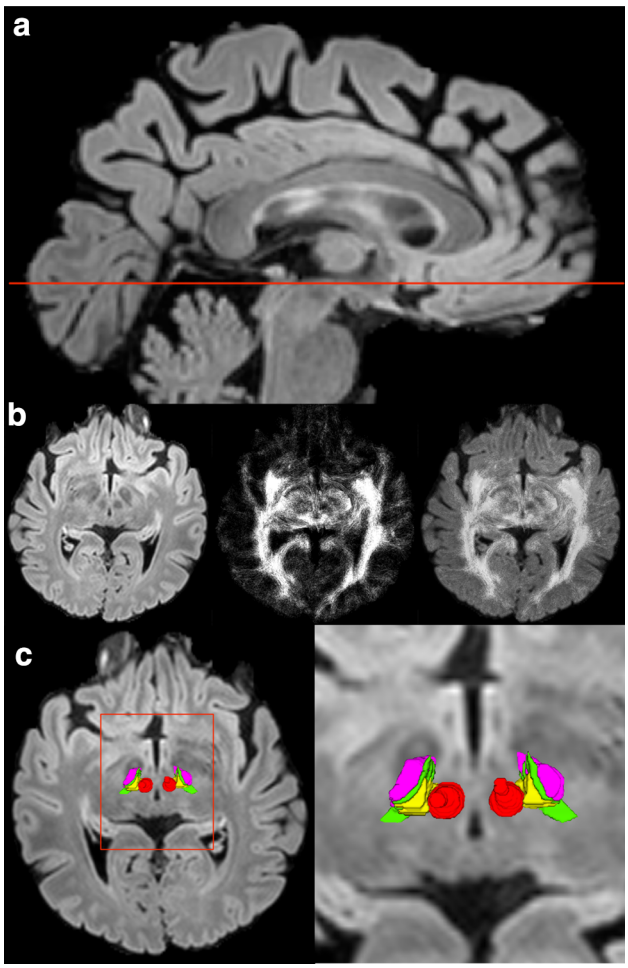

Fig. 1 Segmentation of the PSA in a representative subject. **a** T2FLAIR mid-sagittal slice; the *orange line* indicates the position of the subsequent axial views. **b** Axial slice of T2FLAIR (*left*), TDI (*middle*) and their fusion (*right*). **c** Manual segmentation of the PSA: Ru = *red*, STN = *pink*, Zi = *green*, Raprl = *yellow*. *Orange rectangle* indicates the area that is shown enlarged in the *right panel*. See text for abbreviations

Spurious tractography-derived connections were eliminated using a rigorous statistical method (Morris et al. 2008). Briefly, for each subject the resulting connectivity probability distribution was contrasted to the homologous distribution derived from artificial isotropic FODs with ten times more random streamline samples. A statistical

comparison was made for comparing the empirically computed null connectivity map to the connectivity maps derived from DWI data. Each TDI voxel was considered connected to the Raprl seed only if it had a connection probability of $p < 0.05$ after Bonferroni correction.

A measure of structural connectivity between Raprl and target ROIs was estimated. For each subject, the number of streamlines reaching each anatomic target region was expressed as a percentage (thus the number of streamlines within an anatomic target region represents the proportion) of the total number of streamlines seeded from Raprl.

Results

Volume measurements of Ru and STN were similar to those reported elsewhere (Supplementary TableS1) (Forstmann et al. 2012; Keuken et al. 2013; Massey et al. 2012). We did not find correlations between age and volume measurements of the STN, nor was there any significant inter-hemispheric asymmetry. Co-registration between TDI and T2FLAIR facilitated identification of boundaries of gray matter nuclei and fibers within the PSA, as they take advantage of contrast given by fiber tracking for white matter, and iron deposits for nuclei.

Visual examination of the connectivity of Raprl showed connections with the ipsilateral OFC, PFC, SMA, PMC, globus pallidus (GP), VL, brainstem and bilateral cerebellum, with the majority of fibers traveling close to the midline (Fig. 2). Percentages of structural connectivity of Raprl to target ROIs for each hemisphere are shown in Table 1 (Note that total percentage connectivity for Raprl on each side may surpass 100 %, because some streamlines connect Raprl with a target ROI and continue on to a second target).

Fiber bundles that conform Raprl seem to be intermingled in the PSA, but as they extend beyond and enter the posterior limb of the internal capsule they show a clear spatial organization, with the tracts organized according to their targets, from anterior to posterior as follows: (1) OFC/PFC, (2) GP, (3) SMA and (4) PMC (Fig. 2), with some degree of overlap between fiber populations. Above and below the PSA distinct fiber tracts can be recognized: (1) fibers from the OFC including medial, lateral, polar and subgenual areas extend to the brainstem at the level of the mesencephalic tegmental area; (2) fibers connecting with the GP that divide in the subthalamic area into two groups, one traveling to VL and from here to SMA, while the other group of fibers extends posteriorly and medially to enter Raprl and continues toward the dorsal brainstem; (3) cerebellar fibers continue to the contralateral VL, and segregate into anteriorly and posteriorly located groups; (4) the former continues to travel in the anterior third of the posterior branch of the internal capsule towards the SMA, while the latter component travels in the middle third of the internal capsule towards the PMC.

A description of Raprl connectivity with known anatomical structures follows:

Raprl- OFC and PFC

Tracts related to the medial and lateral OFC are densely grouped within the Raprl, passing near the ventromedial portion of the STN and traveling towards the frontal pole through the anterior limb of the internal capsule (Fig. 3, top panel). Sparse fibers continue to the dorsal pons, some of them going into the ipsilateral cerebellum by the middle cerebellar peduncle and the remaining fibers continuing through the superior medulla oblongata were they disband.

The vast majority of fibers connecting Raprl and PFC reach the rostral middle frontal gyrus and frontal pole, while the connectivity with lateral structures (such as *pars orbitalis*, and *pars triangularis*) is scarce.

GP-Raprl-PPN

On an axial plane, streamlines from the Raprl towards the GP are addressed in an anterior–superior-lateral direction, wrapping the internal capsule nearby its genu, reaching the tip of the internal segment of the GP, as part of the *ansa lenticularis*. A minor component also traverses the internal capsule grasping the ventromedial internal segment of GP area, which corresponds to the *lenticular fasciculus*. The majority of streamlines reach the VL, but sparse tracts appear to continue their trajectory directly towards the frontal pole, motor and premotor cortices. A posterior extension to this bundle goes beyond Forel's fields medial and superior to STN, traverses Raprl and continues medially, posteriorly and inferiorly towards the posterior brainstem (Fig. 3, bottom panel).

All subjects showed connectivity with the dorsal ipsilateral brainstem, and in 83 % of the studied hemispheres that pathway extends an adjacent branch, at the level of the inferior colliculus in the mesencephalic tegmentum, that traverses the midline to the contralateral side, lateral to the brachium conjunctivum (Bcj) and medial to the lemniscal system, in an area that typically corresponds to the anatomic location of the contralateral PPN (Fig. 4).

Raprl-Cerebellum

As shown in Table 1, Raprl connectivity with the ipsilateral cerebellar hemisphere is greater than with the contralateral hemisphere. Contralateral fibers decussate in the Bcj, and both, ipsi and contralateral bundles, reach the red nucleus towards VL in each hemisphere; from here they

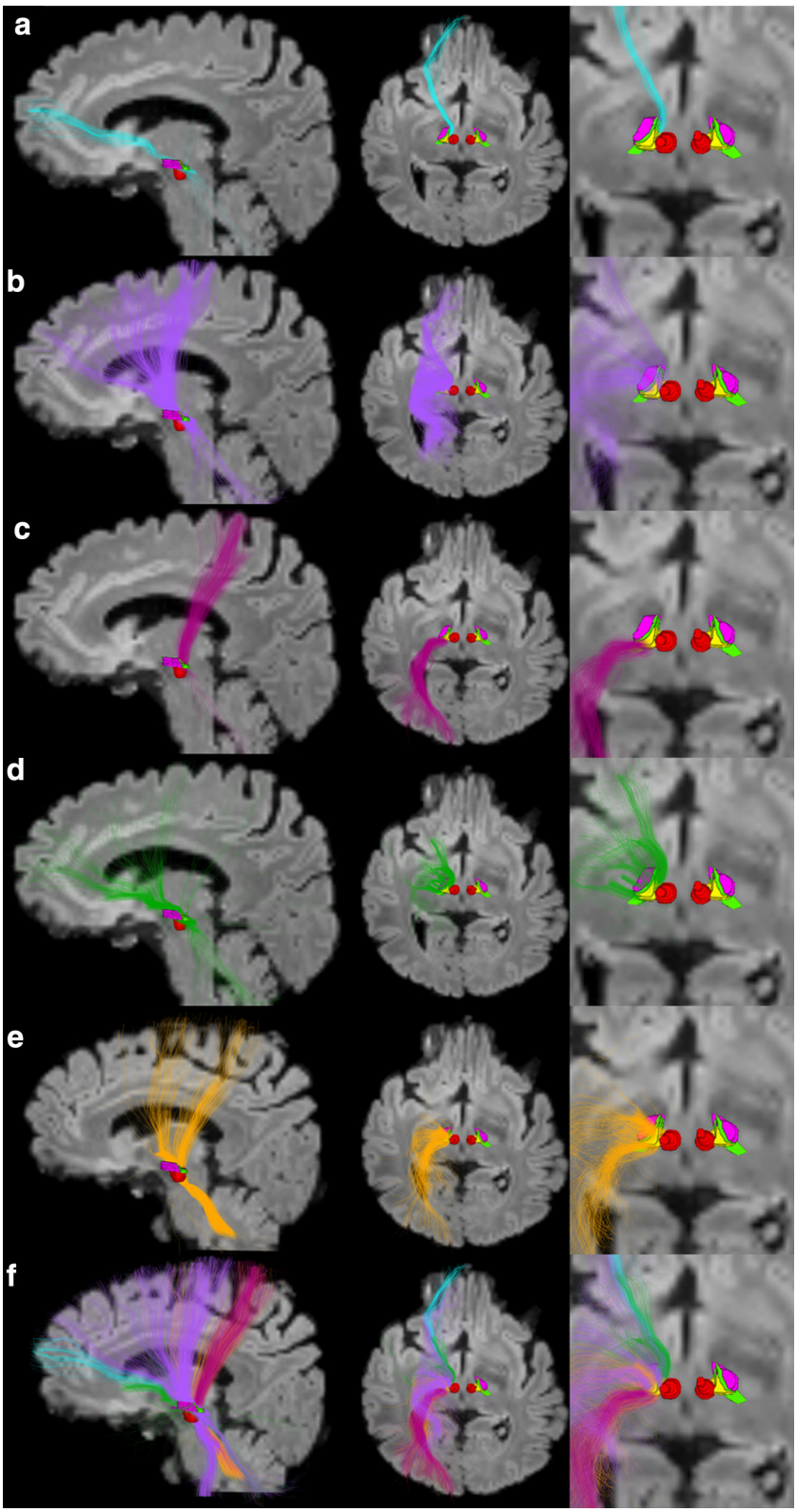

Fig. 2 Probabilistic tractography of Raprl superimposed on a T2FLAIR volume in sagittal and axial planes of a representative subject. *Streamlines* are shown color-coded according to their target: **a** OFC, in *blue*; **b** SMA, in *purple*; **c** PMC, in *pink*; **d** GP, in *green*; **e** cerebellum, in *orange*; **f** all fiber bundles converge at the level of Raprl, yet there is some degree of spatial segregation. *Right-most insets* show an enlarged view of the brainstem, with surface renderings of the manual segmentations of the PSA, *color-coded* as in Fig. 1

continue grouped within the internal capsule as two fiber bundles, the anterior portion reaching the SMA and the posterior subgroup reaching the PMC.

To better define cerebellar connectivity with Raprl, the cerebellum was manually segmented into deep gray nucleus and cortex. The majority of tracts related to the

Table 1 Connectivity percentage (SD) obtained by probabilistic tractography of Raprl with target ROIs in 12 participants

	Raprl left	Raprl right
Thalamus	76.3 % (12.7)	72.4 % (16.4)
GP	4.5 % (3.3)	12.2 % (7.9)
PMC	7.7 % (2.8)	6.3 % (2.5)
SMA	6.2 % (2.2)	6.3 % (3.7)
PFC	2.5 % (1.5)	2.5 % (1.6)
OFC	0.6 % (0.4)	0.4 % (0.3)
Left cerebellar hemisphere	8.5 % (5.4)	2.4 % (2)
Right cerebellar hemisphere	2 % (1.5)	8.8 % (4.5)

Only ipsilateral connections are presented, except for the cerebellum

cerebellar cortex cross the midline through the Bcj, although a few tracts do so through the ventral pons at the level of the middle cerebellar peduncle. Fibers from deep cerebellar nuclei cross the midline only through the superior cerebellar peduncle.

Raprl-SMA and PMC

Pathways connecting the Raprl with SMA and PMC are intermingled at the level of Raprl. Nevertheless, these fibers clearly segregate at the posterior limb of the internal capsule, with tracts related to SMA located more anterior than those reaching PMC throughout their trajectories to the cerebral cortex.

Discussion

Therapeutic implications of PSA connectivity

This study describes the neuroanatomy of the fiber bundles composing the Raprl. The connectivity pattern was highly reliable and reproducible across subjects. We found different fibers systems that converge at this clinically relevant anatomical crossroad: (1) a bundle connecting brainstem with OFC and PFC, (2) a pathway connecting GP with PPN, (3) fibers interconnecting cerebellum with VL and (4) fibers towards motor and premotor cortex.

Lesions and DBS of fibers interconnecting cerebellum, VL and motor cortex have proven to be highly effective for treating tremor of different types and etiologies (Andy et al. 1963; Andy and Jurko 1965; Bertrand et al. 1969; Coenen et al. 2011a, b, 2014; Hamel et al. 2007; Ito 1975; Kitagawa et al. 2005; Murata et al. 2003; Sandvik et al. 2012; Voges et al. 2002). The present report identifies the cerebellar-VL pathway densely grouped in Raprl and further supports the idea that the efficacy of Raprl DBS relies on interference with cerebellar-thalamic-cortical-basal ganglia (BG) connections.

Traditionally, it has been accepted that BG and cerebellum interact through the thalamus and motor cortex. However, recent reports in non-human primates using advanced tracing techniques with neurotropic transneuronal viruses that allows multisynaptic circuits to be traced, revealed that these two systems are directly interconnected (Bostan and Strick 2010; Bostan et al. 2010; Hoshi et al.

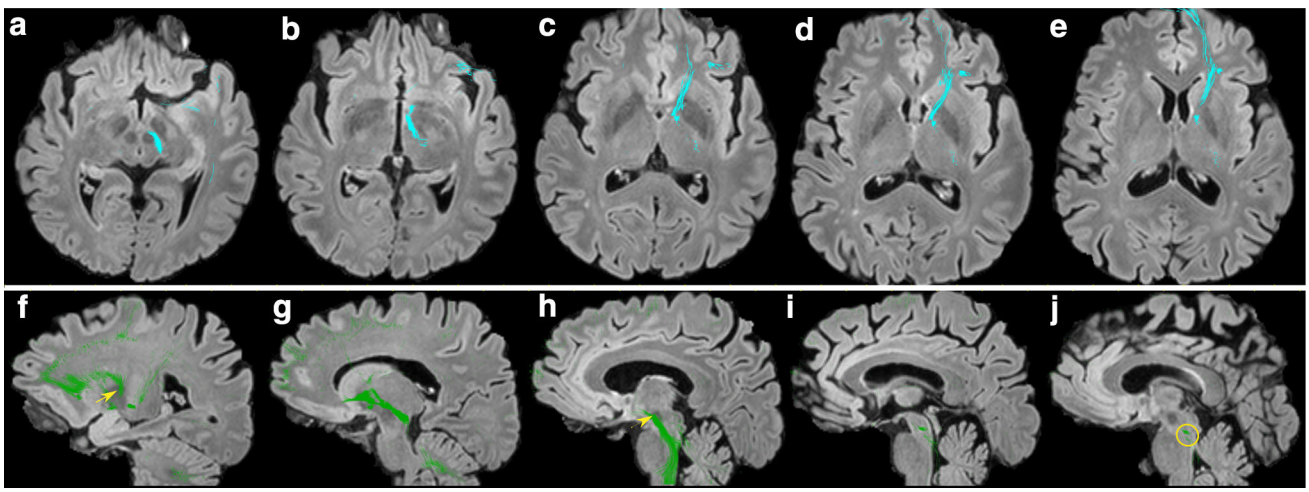

Fig. 3 Probabilistic tractography of Raprl targeting OFC and GP superimposed on a T2FLAIR volume in a representative subject. Axial views in *top panel* (**a**–**e**) show OFC connectivity. Tracts are seen traversing the Raprl (**a**) and the anterior limb of the internal capsule closely related to GP boundaries (**c**–**e**). *Bottom panel* (**f**–**j**) shows sagittal slices spanning from *left* to *right*: (**f**) fibers exit the GP (*arrow*), with some fibers reaching the cerebral cortex, (**g**) fibers enter the subthalamic region and (**h**) continue posteriorly to the dorsal brainstem traversing the Raprl (*arrowhead*). Some fibers traverse the midline (**i**) al the level of the cerebral aqueduct towards the contralateral brainstem (*circled* in **j**)

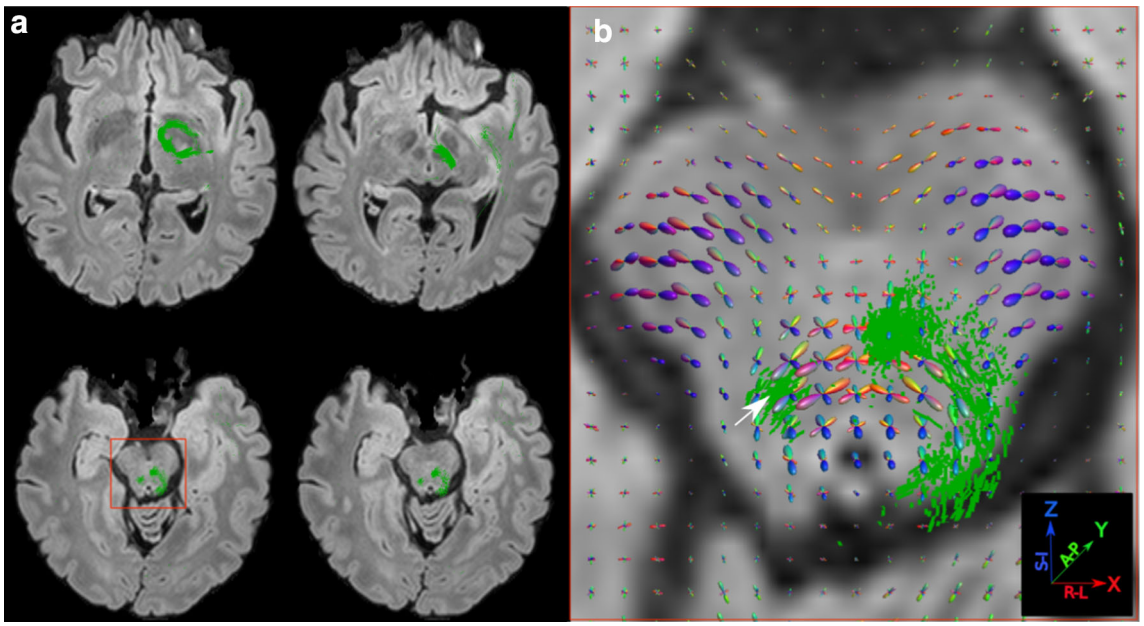

Fig. 4 Tractography of Raprl connecting GP overlaid on axial T2FLAIR images in a representative subject. **a** Superior to inferior axial views show the Raprl connecting GP with ipsi and contralateral PPN. The bundle is seen crossing the midline at the level of the inferior portion of midbrain (*orange box*, enlarged in *panel* **b**). **b** FOD are overlaid on each voxel, demonstrating the complex fiber architecture of this region; the *white arrow* indicates the position of PPN. The FOD glyphs are *color-coded* according to their orientation, as shown in *inset*

2005). These connectivity patterns have been observed in humans using MRI and tractography, supporting dentato-thalamo-striato-pallidal and subthalamo-cerebellar connections (Pelzer et al. 2013). The anatomical connectivity found across all subjects suggests that bundles interconnecting cerebellum and BG go through the PSA, although their role in the physiopathology of tremor is still unclear.

Classical descriptions of cerebellar fibers show their decussation through the Bcj, with few fibers remaining on the ipsilateral side. In this study, however, we found a greater proportion of ipsilateral cerebellar fibers than expected. This could be an artifact of the model for reconstructing probabilistic tractography, as streamlines can more easily propagate on to the ipsilateral side; a similar phenomenon was observed in the tractographic reconstruction of the optic chiasm (Roebroeck et al. 2008).

It is thought that cerebellar fibers project towards the ventral intermedius nucleus (Vim), a target known to selectively control tremor without effect on rigidity, bradykinesia, gait or posture (Benabid et al. 1991); nonetheless, anatomic (Gallay et al. 2008) and tractography (Coenen et al. 2014) studies have demonstrated that cerebellar fibers also project to a more anterior portion of thalamus corresponding to the ventralis oralis posterior nucleus (Vop). In our study a subset of cerebellar fibers project to the same area as GP fibers at the VL, and from here they project to the SMA; this connectivity may be important in treating other symptoms of PD such as rigidity. The SMA plays an important role in preparing motor responses as well as controlling automated motor behavior. DBS in the internal segment of GP and STN induces a decrease in metabolic and regional cerebral blood flow activity of the SMA in patients with PD, which correlates with improvement of rigidity (Fukuda et al. 2001; Karimi et al. 2008).

Raprl-DBS improves both tremor and rigidity (Velasco et al. 2001; Castro et al. 2015), probably because cerebellar thalamic projections ending in Vim and Vop nuclei are packed together in Raprl, with stimulation of the former improving tremor and stimulation of the latter improving rigidity. However, selective improvement of either rigidity or tremor occurs in some patients, indicating that different neuronal circuits are responsible for these symptoms (Castro et al. 2015).

Raprl probabilistic tractography showed a pathway linking GP to PPN; this subthalamic pathway was detected previously by tractography, and was proposed to originate in the STN (Aravamuthan et al. 2007). While STN projections to the PPN are indeed plausible, the present work suggests that there could be a direct pathway from GP to the ipsi and contralateral PPN; to our knowledge, this is the first time that such connection has been demonstrated, and it may explain the improvement in gait reported in clinical studies after DBS of Raprl (Carrillo-Ruiz et al. 2008) and unilateral lesions or DBS on the internal segment of GP (Jiménez et al. 2006).

The bundle relating Raprl to OFC includes frontopolar, subgenual, medial and lateral orbital cortices with the upper mesencephalon. To our knowledge this fiber tract has not been described in humans, but a recent study in macaque monkeys, in which tracers were injected into different frontal cortical regions, found that axons from the ventromedial PFC and OFC travel ventral to the anterior commissure and ventromedial to STN, but most fibers do not enter into the STN (Haynes and Haber 2013). The location of the bundle described in macaques resembles that found here in humans, where the bundle continues posteriorly towards the area of the mesencephalic tegmentum. The physiological importance of this connectivity is unknown, although a cortical control over mesencephalic reticular somatosensory evoked potentials has been proposed as critical in the process of selective attention. Lesions of the PSA in cats (Lindsley et al. 1972) and humans (Velasco and Velasco 1979) selectively block late components of somatosensory evoked potentials related to selective attention (Velasco et al. 1975) and may induce a state of neglect of contralateral extremities (Velasco et al. 1986). On the other hand, metabolic hyperactivity of the OFC is associated with major depression disorder (Drevets 2000) and this hyperactivity decreases when depression is reversed by subgenual frontal DBS, with the degree of improvement related to the precise location of electrodes' contacts used for DBS therapy over OFC fibers (Riva-Posse et al. 2014). On the other hand, inactivation of OFC efferents in animals induces a state of hyperkinesia and behavioral perseverance (Skinner and Lindsley 1973; Velasco et al. 2005), indicating that the OFC exerts a powerful inhibitory influence on mood and motor behavior. From a neuropsychological point of view, PD is related to impairment of executive functions with a substrate in the frontal lobe, including OFC, as revealed by motor and cognitive symptoms, such as gait freezing and instability, as well as emotional apathy and depression. Dysfunction is particularly severe when tests demand fast-rate responses (Dirnberger and Jahanshahi 2013). This "dysexecutive syndrome" may play a role in the pathophysiology of bradykinesia.

The existence in humans of a direct cortico-pallidal pathway has been suggested, linking GP and cortico-frontal pole regions such as 11 and 12 Brodmann's areas (Milardi et al. 2014); and a GABAergic pallido-frontocortical direct pathway was recently described in rats (Chen et al. 2015; Saunders et al. 2015). As seen in the Fig. 2d, the pathway linking Raprl and GP follows a trajectory similar to the one linking Raprl and OFC (Fig. 3a–e), however fibers from the GP are truncated in their way to the frontal pole. Further studies must elucidate the relationship between these two pathways and their possible involvement in the physiopathology of PD.

The connectivity between Raprl and motor and premotor cortex is of great relevance for treatment of PD. A previous optogenetic study in rats concluded that stimulation of the afferents of STN were largely responsible for attenuation of PD symptoms, and the authors proposed that DBS could antidromically recruit neurons located in layer V of PMC (Gradinaru et al. 2009). There are, however, other afferents of the STN such as those from Zi and other axons traveling within Raprl that could contribute to the amelioration of PD symptoms.

Advantages of CSD and TDI

The complex architecture of the brain requires advanced analytical methods to perform tractography. The popular tensor model (Basser and Pierpaoli 1996) is inadequate, as it cannot resolve multiple fiber orientations, which are clearly present in the PSA and beyond, with more than a third of white matter voxels in the entire brain containing crossing fibers (Jeurissen et al. 2013). Tractography based on CSD provided enough information to clearly disentangle the fiber bundles in the PSA. Furthermore, to increase the confidence of the resulting probabilistic tracts, even as they extend away from the seeded region, we used a rigorous statistical approach (Morris et al. 2008) to eliminate any spurious tracts that occur by chance alone. In the present study this statistical method eliminated 0.1 % of the total streamlines that were seeded in TDI $0.2 \times 0.2 \times 0.2$ mm^3 resolution; in our previous study of the same area, in which we seeded the Raprl using the native DWI resolution, 40 %, on average, of the tracts were discarded (García-Gomar et al. 2013). This discrepancy very likely reflects the accuracy of the PSA segmentation in TDI resolution used for perform probabilistic tractography and is in line with the improved tractography of thalamic nuclei derived from TDI (Calamante et al. 2010).

Limitations and future perspectives

Tractographic reconstructions of fiber systems are an indirect measure of true connectivity, and the number of reconstructed tracts is inherently biased by the mathematical models used. We chose to generate streamlines by seeding exclusively at the Raprl, and the resulting streamlines were then grouped according to their targets. This approach allowed for fine precision of seed placement, but it may result in the lack of identification of other potential connections. Therefore, our results should be validated using other methods. Further, we must consider that tractography cannot distinguish the directionality of neural transmission or multisynaptic circuits, thus precluding inferences regarding flow of information and causality. Despite these limitations, tractography is still the

only method for studying anatomical connectivity in humans in vivo and in a non-invasive way, and it is rapidly becoming a valuable tool during neurosurgical planning.

Conclusion

PSA could be adequately segmented with 3T MRI using high-resolution anatomical images and TDI. Probabilistic tractography based on CSD allows the description of the anatomic connectivity of small regions such as Raprl, which is a veritable funnel of several fiber systems that explain, either in isolation or in conjunction, the effect of lesions and DBS of this structure on tremor, rigidity, gait and posture and provide insight about the improvement of bradykinesia. These findings are likely to have implications for neurosurgical planning of ablative procedures or DBS, particulary when coupled with next-generation electrodes that allow directing electrical stimulation to restricted targets (Contarino et al. 2014), tailoring DBS to selected symptoms. Tractography may also be a better method to approach white matter surgical targets within the brain.

Acknowledgments The authors are extremely grateful to participants for their cooperation given. We thank Dr. Laura Chávez Macias and Dr. Monica Madrazo for research assistance, and Dr. Dorothy Pless for proofreading and editing. We thank Dr. Erick Pasaye Alcaraz, Juan Ortiz and the personnel of the Magnetic Resonance Unit for technical assistance. MGGG is a doctoral student from Programa de Doctorado en Ciencias Biomédicas at the Universidad Nacional Autónoma de México (UNAM), and received fellowship 275789 from the National Council of Science and Technology in Mexico (CONACyT). This work was supported by the National Council of Science and Technology in Mexico (CONACyT) from Grant 0114218-2009.

Compliance with ethical standards

Conflict of interest The authors do not have any conflicts of interest.

References

Andy OJ, Jurko MF (1965) Alteration in Parkinso tremor during electrode insertion. Confin Neurol 26:378–381

Andy OJ, Jurko MF, Sias FR (1963) Subthalamotomy in treatment of Parkinsonian tremor. J Neurosurg 20:260–270

Aravamuthan BR, Muthusamy KA, Stein JF, Aziz TZ, Johansen-Berg H (2007) Topography of cortical and subcortical connections of the human pedunculopontine and subthalamic nuclei. NeuroImage 37:694–705. doi:10.1016/j.neuroimage.2007.05.050

Basser PJ, Pierpaoli C (1996) Microstructural and physiological features of tissues elucidated by quantitative-diffusion-tensor MRI. J Magn Reson B 111:209–219

Behrens TEJ, Woolrich MW, Jenkinson M, Johansen-Berg H, Nunes RG, Clare S, Matthews PM, Brady JM, Smith SM (2003) Characterization and propagation of uncertainty in diffusion-weighted MR imaging. Magn Reson Med 50:1077–1088. doi:10.1002/mrm.10609

Benabid AL, Pollak P, Gervason C, Hoffmann D, Gao DM, Hommel M, Perret JE, de Rougemont J (1991) Long-term suppression of tremor by chronic stimulation of the ventral intermediate thalamic nucleus. Lancet 337:403–406

Bertrand C, Hardy J, Molina-Negro P, Martínez N (1969) Optimum physiological target for the arrest of tremor. In: Third Symposium on Parkinson's Disease Edinb Livingstone ES 251–259

Blomstedt P, Sandvik U, Fytagoridis A, Tisch S (2009) The posterior subthalamic area in the treatment of movement disorders: past, present and future. Neurosurgery 64(6):1029–1038. doi:10.1227/01.NEU.0000345643.69486.BC

Blomstedt P, Sandvik U, Linder J, Fredricks A, Forsgren L, Hariz MI (2011) Deep brain stimulation of the subthalamic nucleus versus the zona incerta in the treatment of essential tremor. Acta Neurochir (Wien) 153:2329–2335. doi:10.1007/s00701-011-1157-4

Bostan AC, Strick PL (2010) The cerebellum and basal ganglia are interconnected. Neuropsychol Rev 20:261–270. doi:10.1007/s11065-010-9143-9

Bostan AC, Dum RP, Strick PL (2010) The basal ganglia communicate with the cerebellum. Proc Natl Acad Sci USA 107:8452–8456. doi:10.1073/pnas.1000496107

Calamante F, Tournier J-D, Jackson GD, Connelly A (2010) Track-density imaging (TDI): super-resolution white matter imaging using whole-brain track-density mapping. NeuroImage 53:1233–1243. doi:10.1016/j.neuroimage.2010.07.024

Carrillo-Ruiz JD, Velasco F, Jimènez F, Castro G, Velasco AL, Hernández JA, Ceballos J, Velasco M (2008) Bilateral electrical stimulation of prelemniscal radiations in the treatment of advanced Parkinson's disease. Neurosurgery 62:347–357. doi:10.1227/01.neu.0000316001.03765.e8 **(discussion 357–359)**

Castro G, Carrillo-Ruiz JD, Salcido V, Soto J, García-Gomar MG, Velasco AL, Velasco F (2015) Optimizing prelemniscal radiations as a target for motor symptoms in Parkinson's disease treatment. Stereotact Funct Neurosurg 93:282–291

Chen MC, Ferrari L, Sacchet MD, Foland-Ross LC, Qiu MH, Gotlib IH, Fuller PM, Arrigoni E, Lu J (2015) Identification of a direct GABAergic pallidocortical pathway in rodents. Eur J Neurosci 41(6):748–759. doi:10.1111/ejn.12822

Coenen VA, Allert N, Mädler B (2011a) A role of diffusion tensor imaging fiber tracking in deep brain stimulation surgery: DBS of the dentato-rubro-thalamic tract (drt) for the treatment of therapy-refractory tremor. Acta Neurochir (Wien) 153:1579–1585. doi:10.1007/s00701-011-1036-z **(discussion 1585)**

Coenen VA, Mädler B, Schiffbauer H, Urbach H, Allert N (2011b) Individual fiber anatomy of the subthalamic region revealed with diffusion tensor imaging: a concept to identify the deep brain stimulation target for tremor suppression. Neurosurgery 68:1069–1075. doi:10.1227/NEU.0b013e31820a1a20 **(discussion 1075–1076)**

Coenen VA, Allert N, Paus S, Kronenbürger M, Urbach H, Mädler B (2014) Modulation of the cerebello-thalamo-cortical network in thalamic deep brain stimulation for tremor: a diffusion tensor imaging study. Neurosurgery 75:657–669. doi:10.1227/NEU.0000000000000540 **(discussion 669–670)**

Contarino FM, Bour LJ, Verhagen R, Lourens MAJ, de Bie RMA, Munekhof P, Schuurman PR (2014) Directional steering: a novel approach to deep brain stimulation. Neurology 83:1163–1169. doi:10.1212/WNL.0000000000000823

Den Dunnen WFA, Staal MJ (2005) Anatomical alterations of the subthalamic nucleus in relation to age: a postmortem study. Mov Disord 20:893–898. doi:10.1002/mds.20417

Derogatis LR, Rickels K, Rock AF (1976) The SCL-90 and the MMPI: a step in the validation of a new self-report scale. Br J Psychiatry J Ment Sci 128:280–289

Dirnberger G, Jahanshahi M (2013) Executive dysfunction in Parkinson's disease: a review. J Neuropsychol 7:193–224

Drevets WC (2000) Neuroimaging studies of mood disorders. Biol Psychiatry 48:813–829

Forstmann BU, Keuken MC, Jahfari S, Bazin P-L, Neumann J, Schäfer A, Anwander A, Turner R (2012) Cortico-subthalamic white matter tract strength predicts interindividual efficacy in stopping a motor response. NeuroImage 60:370–375. doi:10.1016/j.neuroimage.2011.12.044

Fukuda M, Mentis MJ, Ma Y, Dhawan V, Antonini A, Lang AE, Lozano AM, Hammerstad J, Lyons K, Koller WC, Moeller JR, Eidelberg D (2001) Networks mediating the clinical effects of pallidal brain stimulation for Parkinson's disease: a PET study of resting-state glucose metabolism. Brain 124:1601–1609

Gallay MN, Jeanmonod D, Liu J, Morel A (2008) Human pallidothalamic and cerebellothalamic tracts: anatomical basis for functional stereotactic neurosurgery. Brain Struct Funct 212:443–463. doi:10.1007/s00429-007-0170-0

García-Gomar MG, Concha L, Alcauter S, Soto Abraham J, Carrillo-Ruiz JD, Castro Farfan G, Velasco CF (2013) Probabilistic tractography of the posterior subthalamic area in Parkinsońs disease patients. J Biomed Sci Eng 6:381–390. doi:10.4236/jbise.2013.63A048

Gradinaru V, Murtaza M, Thompson KR, Henderson JM, Deisseroth K (2009) Optical deconstruction of parkinsonian neural circuitry. Sci NY 324(5925):354–359. doi:10.1126/science.1167093

Hamel W, Fietzek U, Morsnowski A, Schrader B, Herzog J, Weinert D, Pfister G, Müller D, Volkmann J, Deuschl G, Mehdorn HM (2003) Deep brain stimulation of the subthalamic nucleus in Parkinson's disease: evaluation of active electrode contacts. J Neurol Neurosurg Psychiatry 74:1036–1046

Hamel W, Herzog J, Kopper F, Pinsker M, Weinert D, Müller D, Krack P, Deuschl G, Mehdorn HM (2007) Deep brain stimulation in the subthalamic area is more effective than nucleus ventralis intermedius stimulation for bilateral intention tremor. Acta Neurochir. (Wien) 149:749–758. doi:10.1007/s00701-007-1230-1 **(discussion 758)**

Haynes WIA, Haber SN (2013) The organization of prefrontal-subthalamic inputs in primates provides an anatomical substrate for both functional specificity and integration: implications for Basal Ganglia models and deep brain stimulation. J Neurosci 33:4804–4814. doi:10.1523/JNEUROSCI.4674-12.2013

Herzog J, Fietzek U, Hamel W, Morsnowski A, Steigerwald F, Schrader B, Weinert D, Pfister G, Müller D, Mehdorn HM, Deuschl G, Volkmann J (2004) Most effective stimulation site in subthalamic deep brain stimulation for Parkinson's disease. Mov Disord 19:1050–1054. doi:10.1002/mds.20056

Herzog J, Hamel W, Wenzelburger R, Pötter M, Pinsker MO, Bartussek J, Morsnowski A, Steigerwald F, Deuschl G, Volkmann J (2007) Kinematic analysis of thalamic versus subthalamic neurostimulation in postural and intention tremor. Brain 130:1608–1625. doi:10.1093/brain/awm077

Hoshi E, Tremblay L, Féger J, Carras PL, Strick PL (2005) The cerebellum communicates with the basal ganglia. Nat Neurosci 8:1491–1493. doi:10.1038/nn1544

Ito Z (1975) Stimulation and destruction of the prelemniscal radiation or its adjacent area in various extrapyramidal disorders. Confin Neurol 37:41–48

Jeurissen B, Leemans A, Tournier J-D, Jones DK, Sijbers J (2013) Investigating the prevalence of complex fiber configurations in white matter tissue with diffusion magnetic resonance imaging. Hum Brain Map 34:2747–2766. doi:10.1002/hbm.22099

Jiménez F, Velasco F, Velasco M, Brito F, Morel C, Márquez I, Pérez ML (2000) Subthalamic prelemniscal radiation stimulation for the treatment of Parkinson's disease: electrophysiological characterization of the area. Arch Med Res 31:270–281

Jiménez F, Velasco F, Carrillo-Ruiz JD, García L, Madrigal A, Velasco AL, Márquez I (2006) Comparative evaluation of the effects of unilateral lesion versus electrical stimulation of the globus pallidus internus in advanced Parkinson's disease. Stereotact Funct Neurosurg 84:64–71. doi:10.1159/000094034

Karimi M, Golchin N, Tabbal SD, Hershey T, Videen TO, Wu J, Usche JWM, Revilla FJ, Hartlein JM, Wernle AR, Mink JW, Perlmutter JS (2008) Subthalamic nucleus stimulation-induced regional blood flow responses correlate with improvement of motor signs in Parkinson disease. Brain 131:2710–2719. doi:10.1093/brain/awn179

Kerl HU, Gerigk L, Huck S, Al-Zghloul M, Groden C, Nölte IS (2012) Visualisation of the zona incerta for deep brain stimulation at 3.0 Tesla. Clin Neuroradiol 22:55–68. doi:10.1007/s00062-012-0136-3

Kerl HU, Gerigk L, Brockmann MA, Huck S, Al-Zghloul M, Groden C, Hauser T, Nagel AM, Nölte IS (2013) Imaging for deep brain stimulation: the zona incerta at 7 Tesla. World J Radiol 5:5–16. doi:10.4329/wjr.v5.i1.5

Keuken MC, Bazin P-L, Schäfer A, Neumann J, Turner R, Forstmann BU (2013) Ultra-high 7T MRI of structural age-related changes of the subthalamic nucleus. J Neurosci 33:4896–4900. doi:10.1523/JNEUROSCI.3241-12.2013

Kitagawa M, Murata J, Uesugi H, Kikuchi S, Saito H, Tashiro K, Sawamura Y (2005) Two-year follow-up of chronic stimulation of the posterior subthalamic white matter for tremor-dominant Parkinson's disease. Neurosurgery 56:281–289 **(discussion 281–289)**

Kitajima M, Korogi Y, Kakeda S, Moriya J, Ohnari N, Sato T, Hayashida Y, Hirai T, Okuda T, Yamashita Y (2008) Human subthalamic nucleus: evaluation with high-resolution MR imaging at 3.0 T. Neuroradiology 50:675–681. doi:10.1007/s00234-008-0388-4

Leemans A, Jones DK (2009) The B-matrix must be rotated when correcting for subject motion in DTI data. Magn Reson Med 61:1336–1349. doi:10.1002/mrm.21890

Lindsley DF, Ranf SK, Barton RJ (1972) Corticofugal influences on reticular formation evoked activity in cats. Exp Neurol 34:511–521

Massey LA, Miranda MA, Zrinzo L, Al-Helli O, Parkes HG, Thornton JS, So P-W, White MJ, Mancini L, Strand C, Holton JL, Hariz MI, Lees AJ, Revesz T, Yousry TA (2012) High resolution MR anatomy of the subthalamic nucleus: imaging at 9.4 T with histological validation. NeuroImage 59:2035–2044. doi:10.1016/j.neuroimage.2011.10.016

Milardi D, Gaeta M, Marino S, Arrigo A, Vaccarino G, Mormina E, Rizzo G, Milazzo C, Finocchio G, Baglieri A, Anastasi G, Quartarone A (2014) Basal ganglia network by constrained spherical deconvolution: a possible cortico-pallidal pathway?. Disord Off J Mov Disord Soc, Mov. doi:10.1002/mds.25995

Morris DM, Embleton KV, Parker GJM (2008) Probabilistic fibre tracking: differentiation of connections from chance events. NeuroImage 42:1329–1339. doi:10.1016/j.neuroimage.2008.06.012

Mundinger F (1965) Stereotactic interventions on the zona incerta for treatment of extrapyramidal motor disturbances. Confin Neurol 26:222–230

Murata J, Kitagawa M, Uesugi H, Saito H, Iwasaki Y, Kikuchi S, Tashiro K, Sawamura Y (2003) Electrical stimulation of the posterior subthalamic area for the treatment of intractable proximal tremor. J Neurosurg 99:708–715. doi:10.3171/jns.2003.99.4.0708

Oldfield RC (1971) The assessment and analysis of handedness: the Edinburgh inventory. Neuropsychologia 9:97–113

Pelzer EA, Hintzen A, Goldau M, von Cramon DY, Timmermann L, Tittgemeyer M (2013) Cerebellar networks with basal ganglia:

feasibility for tracking cerebello-pallidal and subthalamo-cerebellar projections in the human brain. Eur J Neurosci 38:3106–3114. doi:10.1111/ejn.12314

Plaha P, Patel NK, Gill SS (2004) Stimulation of the subthalamic region for essential tremor. J Neurosurg 101:48–54. doi:10.3171/jns.2004.101.1.0048

Riva-Posse P, Choi KS, Holtzheimer PE, McIntyre CC, Gross RE, Chaturvedi A, Crowell AL, Garlow SJ, Rajendra JK, Mayberg HS (2014) Defining critical white matter pathways mediating successful subcallosal cingulate deep brain stimulation for treatment-resistant depression. Biol Psychiatry 76:963–969. doi:10.1016/j.biopsych.2014.03.029

Roebroeck A, Galuske R, Formisano E, Chiry O, Bratzke H, Ronen I, Kim D, Goebel R (2008) High-resolution diffusion tensor imaging and tractography of the human optic chiasm at 9.4 T. NeuroImage 39:157–168. doi:10.1016/j.neuroimage.2007.08.015

Sandvik U, Koskinen L-O, Lundquist A, Blomstedt P (2012) Thalamic and subthalamic deep brain stimulation for essential tremor: where is the optimal target? Neurosurgery 70:840–845. doi:10.1227/NEU.0b013e318236a809 **(discussion 845–846)**

Saunders A, Oldenburg IA, Berezovskii VK, Johnson CA, Kingery ND, Elliott HL, Xie T, Gerfen CR, Sabatini BL (2015) A direct GABAergic output from the basal ganglia to the frontal cortex. Nature 521(7550):85–89. doi:10.1038/nature14179

Schaltenbrand G, Wahren W (1977) Atlas for stereotaxy of the human brain, 2nd edn. Stuttgart, Thieme

Skinner JE, Lindsley DB (1973) The non-specific mediothalamic-frontocortical sys- tem: its influence in electrocortical activity and behavior. In: Pribram KH, Luria AR (eds) Psychophysiology of frontal lobes. Academic Press, New York, pp 185–236

Spiegel EA, Wycis HT, Szekely EG, Baird HW, Adams J, Flanagan M (1962) Campotomy. Trans Am Neurol Assoc 87:240–242

Tournier J-D, Calamante F, Connelly A (2007) Robust determination of the fibre orientation distribution in diffusion MRI: non-negativity constrained super-resolved spherical deconvolution. NeuroImage 35:1459–1472. doi:10.1016/j.neuroimage.2007.02.016

Tournier J-D, Yeh C-H, Calamante F, Cho K-H, Connelly A, Lin C-P (2008) Resolving crossing fibres using constrained spherical deconvolution: validation using diffusion-weighted imaging phantom data. NeuroImage 42:617–625. doi:10.1016/j.neuroimage.2008.05.002

Tournier J-D, Calamante F, Connelly A (2012) MRtrix: diffusion tractography in crossing fiber regions. Int J Imaging Syst Technol 22:53–66. doi:10.1002/ima.22005

Velasco F, Velasco M (1979) A reticulothalamic system mediating proprioceptive attention and tremor in man. Neurosurgery 4:30–36

Velasco FC, Molina-Negro P, Bertrand C, Hardy J (1972) Further definition of the subthalamic target for arrest of tremor. J Neurosurg 36:184–191. doi:10.3171/jns.1972.36.2.0184

Velasco M, Velasco F, Maldonado H, Machado JP (1975) Differential effect of thalamic and subthalamic lesions on early and late components of the somatic evoked potentials in man. Electroencephalogr Clin Neurophysiol 39:163–171

Velasco F, Velasco M, Ogarrio C, Olvera A (1986) Neglect induced by thalamotomy in humans: a quantitative appraisal of the sensory and motor deficits. Neurosurgery 19:744–751

Velasco F, Jiménez F, Pérez ML, Carrillo-Ruiz JD, Velasco AL, Ceballos J, Velasco M (2001) Electrical stimulation of the prelemniscal radiation in the treatment of Parkinson's disease: an old target revised with new techniques. Neurosurgery 49:293–306 **(discussion 306–308)**

Velasco F, Velasco M, Jiménez F, Velasco AL, Salin-Pascual R (2005) Neurobiological background for performing surgical intervention in the inferior thalamic peduncle for treatment of major depression disorders. Neurosurgery 57:439–448 **(discussion 439–448)**

Voges J, Volkmann J, Allert N, Lehrke R, Koulousakis A, Freund H-J, Sturm V (2002) Bilateral high-frequency stimulation in the subthalamic nucleus for the treatment of Parkinson disease: correlation of therapeutic effect with anatomical electrode position. J Neurosurg 96:269–279. doi:10.3171/jns.2002.96.2.0269

Volkmann J (2004) Deep brain stimulation for the treatment of Parkinson's disease. J Clin Neurophysiol 21:6–17

Wichmann T, Delong MR (2011) Deep-brain stimulation for basal ganglia disorders. Basal Ganglia 1:65–77. doi:10.1016/j.baga.2011.05.001